All-Metallic ε-Near-Zero (ENZ) Lens Based On Ultra-Narrow Hollow Rectangular Waveguides: Experimental Results

B. Orazbayev, V. Torres, V. Pacheco-Peña, F. Falcone, J. Teniente, M. Beruete, M.Sorolla
Dept. of Electrical and Electronic Engineering
Antennas Group – TERALAB, Universidad Pública de Navarra
Pamplona, Spain
b.orazbayev@unavarra.es
victor.torres@unavarra.es
victor.pacheco@unavarra.es
francisco.falcone@unavarra.es
jorge.teniente@unavarra.es
miguel.beruete@unavarra.es

M. Navarro-Cía
Dept. of Electrical and Electronic Engineering Optical and Semiconductor Devices Group, Imperial College London
London SW7 2BT, United Kingdom
Centre for Plasmonics and Metamaterials, Imperial College London
London SW7 2AZ, United Kingdom
Centre for Terahertz Science and Engineering, Imperial College London
London SW7 2AZ, United Kingdom
m.navarro@imperial.ac.uk

N. Engheta
Dept. Electrical and Systems Engineering, University of Pennsylvania, 200 South 33rd Street, ESE 203
Moore, Philadelphia, Pennsylvania 19104, USA
engheta@ee.upenn.edu

Abstract—Here we perform numerical and experimental investigation of plano-concave all-metallic ε-near-zero (ENZ) lens with operational frequency f = 144 GHz. The ENZ lens is achieved by stacking an array of narrow hollow rectangular waveguides working near cut-off frequency. Focusing and radiation properties are numerically analyzed and measured. The enhancement of 5.61 dB and directivity of 17.6 dBi are shown. Good agreement between experimental and numerical results is demonstrated.

Keywords—metamaterial lenses; ENZ media; millimeter waves

I. INTRODUCTION

For many years control of the transmission of light has been an important challenge. For instance, conventional dielectric lenses have been used to collimate light for centuries. However, due to the limited range of permittivity and permeability of natural materials, these lenses are often bulky and have limited range of applications. In recent years, appearance of metamaterials produced significant shift in the solution of this problem. Metamaterials, whose values of permittivity (ε) or permeability (μ) can be designed at will, have been proposed to many applications, such as negative refraction, lenses, cloaking devices or even computational metamaterials [1]–[6].

More recently, metamaterials with an effective permittivity close to zero have gained interest, since they offer new exciting possibilities, such as supercoupling or energy squeezing [7]. Such ENZ materials make possible, under certain conditions (simultaneous relative permeability close to zero or cross-sectional area electrically very small), to match bulk metamaterial impedance to free space and also provide small phase advance over a physically long distance for propagating

electromagnetic waves in these media [7]. Based on these properties several different applications have been proposed [8]–[12].

A practical implementation of ENZ metamaterials is based on stacking perfectly electric conducting (PEC) metallic waveguides working at frequency close to cut-off frequency. In this communication, using such implementation, all-metallic ENZ lens is designed, fabricated and measured at frequency 144 GHz [13]. Along with the transmission properties, the radiation characteristics are analyzed.

II. LENS DESIGN

The ENZ plano-concave lens is realized by employing a two-dimensional array of narrow hollow rectangular waveguides of dimensions h_x and h_y, along x and y axes, where $h_y << h_x$. The aperture dimension perpendicular to the electric field excitation is h_x = 1.1±0.025mm with the aim to have the cutoff frequency of the fundamental mode TE_{10} at 136.36 GHz. In order to have energy squeezing or bulk material impedance matched with free space, the dimension h_y must be electrically very small [14], so it is designed with a value h_y = 0.05 ± 0.02mm ≈ λ_0/42. The final design of whole ENZ lens consists of an array of 33 × 144 narrow hollow rectangular waveguides along x and y axes, respectively, with total dimensions d_x = 46.2 mm, d_y = 55.5 mm and L_z = 40 mm. The total size of the lens excluding top and bottom bases is L_x = 76.2 mm, L_y = 86.2 mm and L_z = 40 mm. Fabricated prototype is presented in Fig. 1. Due to the small phase variation in ENZ media, the phase front is conformal to the exit surface [15], [16]. Thus, the output face should have concave profile in order to focus an incoming plane wave. Following these principles, the ENZ lens is designed and fabricated with a flat face at input and a

concave profiled face with diameter $d_y = 55.5$ mm at the output.

III. RESULTS

A. Focusing properties

The performance of ENZ lens was experimentally characterized by means of an Agilent Technologies N5242A PNA-X network analyzer. A scheme of experimental setup is shown in Fig. 2(a). A D-band corrugated horn antenna generating a y-polarized Gaussian beam was used as a source, placed 160 mm away from the flat face of the lens. A waveguide probe WR-8.0 was used as a receiver, which was fixed on a motorized 2-axis translation stage. Raster scanning was done with a minimum step of 0.8 mm in both x and y axes in a rectangle of 320 mm × 320 mm which was 100 mm away from output of the lens. Both transmitter and receiver were connected to the Agilent VNA. The setup was covered with millimeter-wave absorbers with aim to minimize undesired reflections and scattering. A spatial field distribution in any xy plane can be obtained from the measured components of the electric field by plane-to-plane translation, performed with fast Fourier transformation [17].
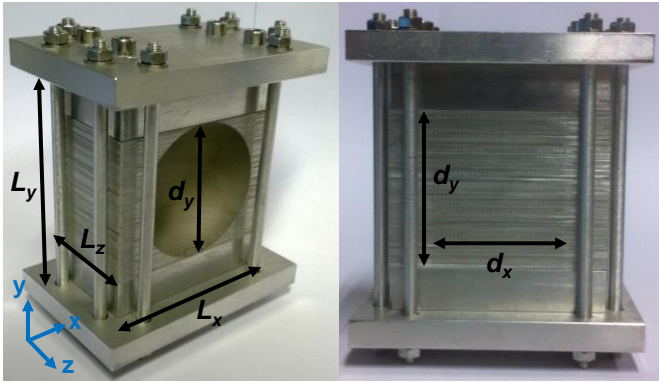

Fig. 1. Photograph of the plano-concave ENZ metallic lens.

First, in order to obtain the operational frequency of ENZ lens the experimental transmission enhancement spectra along the optical z-axis were obtained (Fig. 2(b) right inset). As it can be observed in this figure the maximum transmission occurs at 144 GHz. At this frequency effective permittivity $\varepsilon_{eff} = 0.103$ is close to zero, accomplishing the condition of ENZ media and therefore it will be considered as working frequency. The focal length at this frequency is $z = 40.4$ mm.

For the purpose of comparison a numerical characterization of realistic 3D model of ENZ lens is done by means of the commercial software CST Microwave Studio™ using the transient solver. The whole 3D model is built according to fabrication dimensions, including the bases on the top and bottom but excluding the crosspieces. Simulations results for transmission enhancement spectra along the optical z-axis are presented in the left panel of Fig. 2 (b). It can be noticed a slight frequency shift in the response, which is attributed to fabrication tolerances. At operational frequency the focal length is 38.91 mm, which is in good agreement with experimental results.

Next, the xy-plane scanning was done at the position of the focal length z = 40.4 mm. The experimental normalized transmission enhancement is shown in Fig. 3 (b) where a clear focus can be observed. The measured maximum value of transmission enhancement is 5.61 dB. The same results for simulations are shown in Fig. 3 (a). However, the maximum transmission enhancement is 16.77 dB, which is significantly higher than in the experiment. This disagreement may be due to the non-uniform illumination of the lens in the experiment, resulting in the transmission reduction [18].

The experimental and simulation results of the transmission along x- and y-axes at the each focal plane are plotted in Fig. 3 (c). Experimentally, the full width at half maximum (FWHM) is $2.21\lambda_0$ and $1.69\lambda_0$ for x- and y-plane respectively. For simulations FWHM is $0.78\lambda_0$ and $0.79\lambda_0$ for x- and y-plane respectively. It must be highlighted that the secondary lobes along the x-axis are higher than those along the y-axis. This is related with the effective aperture because, as described in the design section, the waveguide array is shorter along the x-axis causing the effective length to be 17% lower than the y-axis ($d_y > d_x$), and therefore, the energy focusing is worse along x. The value of depth of focus (DoF) is 14.8 mm = 7.11 λ_0 obtained in the experiment. In the simulation DoF is 3.94 mm = 1.9 λ_0. For ease of comparison all values are presented in Table 1.
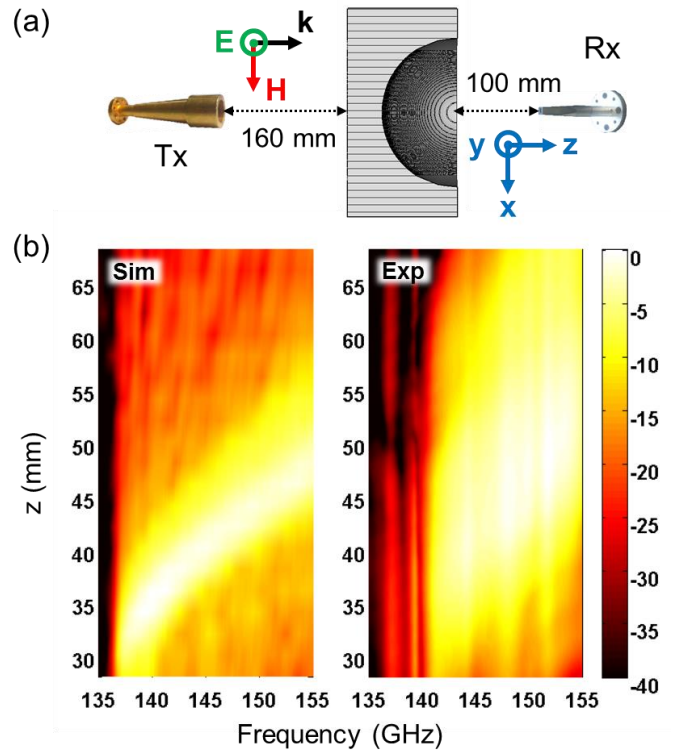

Fig. 2. (a) Sketch of the experimental set-up. (b) Normalized transmission enhancement spectra along the optical z-axis: (left) simulation, (right) measurement.

B. Radiation characteristics

To complete our study, the analysis of radiation properties was performed. A sketch of the experimental setup is shown in Fig. 4 (a). A waveguide probe WR-5.1 was placed at the experimental focus and used as a source while a waveguide

probe WR-8.0 was used as a detector. A raster scanning was done in a rectangle of 200 mm × 200 mm with a step of 0.8 mm at 100 mm away from the exit face of the lens.
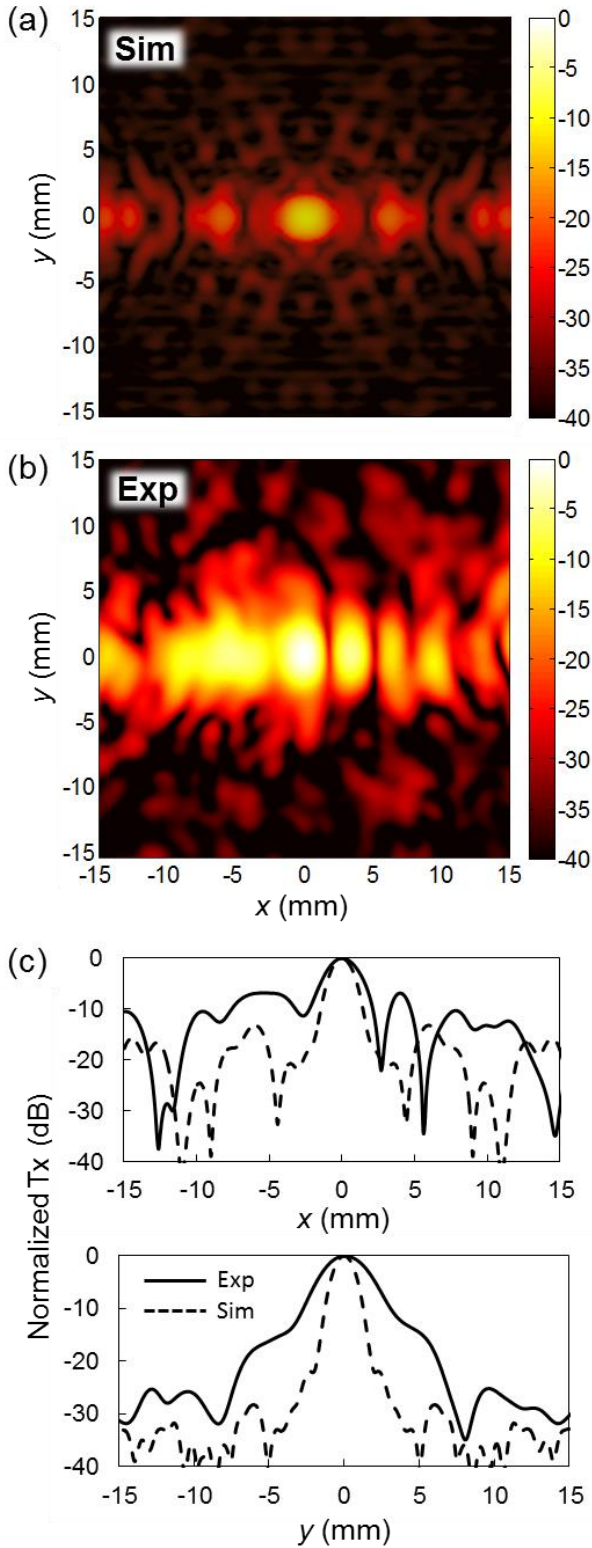

TABLE I
SUMMARY OF THE FOCUS PERFORMANCE

	FL[a]	DoF[b]	FWHM[c]		Max. Tx.[d]
			x-axis	y-axis	
Exp	40.40 mm	14.8 mm $7.11\lambda_0$	2.36 mm $1.13\lambda_0$	3.04 mm $1.46\lambda_0$	5.61 dB
Sim	38.91 mm	4.59 mm $2.21\lambda_0$	1.63 mm $0.78\lambda_0$	1.45 mm $0.69\lambda_0$	16.77 dB

[a]FL is the focal length
[b]DoF is the depth of focus
[c]FWHM is the full-width at half-maximum
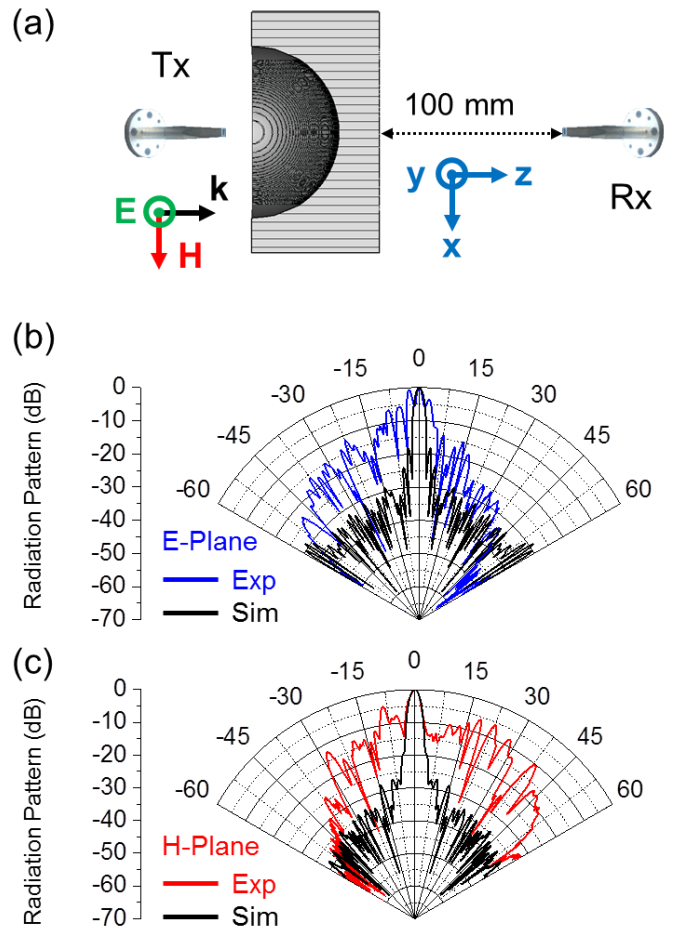[d]Max. Tx. is the maximum transmission enhancement

Fig. 4. (a) Sketch of the experimental set-up used for the far-field characterization. Measured and simulated co-polar radiation pattern on the E-plane (b) and H-plane (c).

Fig. 3. (a) Simulated and (b) measured on the *xy*-plane normalized transmission enhancement at the working frequency f_0= 144 GHz. (c) Normalized transmission at f_0 along the *x*-axis (top) and along the y-axis (bottom) at the FL.

To obtain the radiation pattern the planar near-field to far-field transformation was applied, which allows transforming the measured fields in this rectangle to the far-field region [17]. In the simulation only the end of the WR-8.0 is included and the radiation pattern is obtained by a far-field monitor.

In Fig. 4 (b,c) simulation and experimental results are shown for E- and H-plane, respectively. On the E-plane (Fig. 5(b)) experimental results demonstrate a narrow main lobe with a half-power beamwidth (HPBW) of 1.6 deg and first null beam width (FNBW) equal to 2.8 deg. In the simulation a main lobe is obtained with a HPBW and FNBW of 2.2 deg and 5.6 deg, respectively. In the experimental radiation pattern secondary lobes are higher than in the simulation that can be tied to undesired effect of the probe WR-5.1. In the experiment the first side-lobe levels (FSLL) are -3.6 dB and -0.8 dB while in the simulation FSLL is -18.3 dB at both sides of the main lobe. On the H-plane (Fig. 5(c)) experimental results are presented with HPBW=3.0 deg and FNWB=8.2 deg, which is in very good agreement with the simulated values of HPBW=2.9 deg and FNWB=7.8 deg. The level of the secondary lobes is much lower: -13.8 dB and -7.8 dB for experimental results, and -19.3 dB for the simulation. The measured directivity is equal to 17.6 dBi, and 25.4 dBi in the simulation. All these results are presented in Table II.

TABLE II
RADIATION PATTERN PARAMETERS

	HPBW[a]		FNBW[b]		FSLL[c]		Directivity
	E-Plane	H-Plane	E-Plane	H-Plane	E-Plane	H-Plane	
Exp	1.6 deg	3.0 deg	2.3 deg	8.2 deg	-3.6 dB	-13.8 dB	17.6 dBi
Sim	2.2 deg	2.9 deg	5.6 deg	7.8 deg	-18.3 dB	-19.3 dB	25.4 dBi

[a]HPBW is the half-power beamwidth
[b]FNBW is the first null beam width
[c]FSLL is the first side-lobe level

IV. CONCLUSIONS

In this work, an ENZ lens with a plano-concave profile has been designed, fabricated and demonstrated experimentally. The design consist of a 2D array of narrow hollow rectangular waveguides working near the cutoff frequency $f_0 = 144$ GHz of the fundamental mode TE_{10}. Experimental results show a good agreement with simulation results. A focal length found at $z = 40.4$ mm and $z = 38.91$ mm for experimental and simulation, respectively. The effective permittivity of the lens at the operational frequency in the experiment 144 GHz is 0.103, demonstrating that the lens mimics a medium with permittivity near zero. For the working frequency the measured directivity is equal to 17.6 dBi. The ENZ lens presented in this work demonstrates possibilities of using waveguide-based ENZ metamaterials in applications such as graded-index lenses, prisms or beam steerers.

REFERENCES

[1] R. A. Shelby, D. R. Smith, and S. Schultz, "Experimental verification of a negative index of refraction.," *Science*, vol. 292, no. 5514, pp. 77–9, Apr. 2001.

[2] V. M. Shalaev, "Optical negative-index metamaterials," *Nat. Photonics*, vol. 1, no. 1, pp. 41–48, Jan. 2007.

[3] Z. Liu, H. Lee, Y. Xiong, C. Sun, and X. Zhang, "Far-field optical hyperlens magnifying sub-diffraction-limited objects.," *Science*, vol. 315, no. 5819, p. 1686, Mar. 2007.

[4] M. Silveirinha, A. Alù, and N. Engheta, "Parallel-plate metamaterials for cloaking structures," *Phys. Rev. E*, vol. 75, no. 3, p. 036603, Mar. 2007.

[5] A. Silva, F. Monticone, G. Castaldi, V. Galdi, A. Alù, and N. Engheta, "Performing mathematical operations with metamaterials.," *Science*, vol. 343, no. 6167, pp. 160–3, Jan. 2014.

[6] A. Demetriadou and Y. Hao, "Slim Luneburg lens for antenna applications.," *Opt. Express*, vol. 19, no. 21, pp. 19925–34, Oct. 2011.

[7] M. Silveirinha and N. Engheta, "Tunneling of Electromagnetic Energy through Subwavelength Channels and Bends using ε-Near-Zero Materials," *Phys. Rev. Lett.*, vol. 97, no. 15, p. 157403, Oct. 2006.

[8] A. Alù, M. G. Silveirinha, A. Salandrino, and N. Engheta, "Epsilon-near-zero metamaterials and electromagnetic sources : Tailoring the radiation phase pattern," pp. 1–13, 2007.

[9] B. Edwards, A. Alù, M. Silveirinha, and N. Engheta, "Experimental Verification of Plasmonic Cloaking at Microwave Frequencies with Metamaterials," *Phys. Rev. Lett.*, vol. 103, no. 15, p. 153901, Oct. 2009.

[10] A. Monti, F. Bilotti, A. Toscano, and L. Vegni, "Possible implementation of epsilon-near-zero metamaterials working at optical frequencies," *Opt. Commun.*, vol. 285, no. 16, pp. 3412–3418, Jul. 2012.

[11] C. Argyropoulos, P.-Y. Chen, G. D'Aguanno, N. Engheta, and A. Alù, "Boosting optical nonlinearities in ε-near-zero plasmonic channels," *Phys. Rev. B*, vol. 85, no. 4, p. 045129, Jan. 2012.

[12] N. Engheta, "Circuits with light at nanoscales: optical nanocircuits inspired by metamaterials.," *Science*, vol. 317, no. 5845, pp. 1698–702, Sep. 2007.

[13] V. Torres, B. Orazbayev, V. Pacheco-Peña, J. Teniente, M. Beruete, M. Navarro-Cía, M. Sorolla, and N. Engheta, "Experimental Demonstration of a Millimeter-Wave Metallic ENZ Lens based on the Energy Squeezing Principle," *submitted*.

[14] M. Silveirinha and N. Engheta, "Theory of supercoupling, squeezing wave energy, and field confinement in narrow channels and tight bends using ε near-zero metamaterials," *Phys. Rev. B*, vol. 76, no. 24, p. 245109, Dec. 2007.

[15] A. Alù, M. Silveirinha, A. Salandrino, and N. Engheta, "Epsilon-near-zero metamaterials and electromagnetic sources: Tailoring the radiation phase pattern," *Phys. Rev. B*, vol. 75, no. 15, p. 155410, Apr. 2007.

[16] M. Navarro-Cía, M. Beruete, M. Sorolla, and N. Engheta, "Lensing system and Fourier transformation using epsilon-near-zero metamaterials," *Phys. Rev. B*, vol. 86, no. 16, p. 165130, Oct. 2012.

[17] S. Gregson, J. McCormick, and C. Parini, *Principles of Planar Near-Field Antenna Measurements*. 2007.

[18] V. Torres, V. Pacheco-Peña, P. Rodríguez-Ulibarri, M. Navarro-Cía, M. Beruete, M. Sorolla, and N. Engheta, "Terahertz epsilon-near-zero graded-index lens.," *Opt. Express*, vol. 21, no. 7, pp. 9156–66, Apr. 2013.